Thermochimica Acta 496 (2009) 156–160

Contents lists available at ScienceDirect

Thermochimica Acta

journal homepage: www.elsevier.com/locate/tca

Synthesis, characterization and thermal behaviour on solid tartrates of some bivalent metal ions

Emanuel C. Rodrigues[a,*], Claudio T. Carvalho[b], Adriano B. de Siqueira[c], Gilbert Bannach[d], Massao Ionashiro[b]

[a] Centro Universitário da Fundação Educacional de Barretos, UNIFEB, CEP 14780-226, Barretos, SP, Brazil
[b] Instituto de Química, UNESP, C.P. 355, CEP 14801-970, Araraquara, SP, Brazil
[c] Universidade Federal do Mato Grosso, UFMT, CEP 78698-000, Cuiabá, MT, Brazil
[d] Instituto de Química de São Carlos, USP, CEP 13560-970, São Carlos, SP, Brazil

ARTICLE INFO

Article history:
Received 26 May 2009
Received in revised form 9 July 2009
Accepted 24 July 2009
Available online 3 August 2009

Keywords:
Bivalent metals
Tartrate
Characterization
Thermal behaviour

ABSTRACT

Solid-state M–L compounds, where M stands for bivalent Mn, Fe, Co, Ni, Cu, Zn and L is tartrate, have been synthesized. Thermogravimetry and differential thermal analysis (TG–DTA), differential scanning calorimetry (DSC), X-ray powder diffractometry, infrared spectroscopy, elemental analysis and complexometry were used to characterize and to study the thermal behaviour of these compounds. The TG–DTA and DSC curves show that the manganese, cobalt and nickel compounds are hydrated while iron, copper and zinc ones are anhydrous. The thermal stability of the anhydrous compounds depends on the nature of the metal ion, and it follows the order: Zn > Cu > Mn = Co > Ni > Fe. These curves also show that the thermal decomposition occurs in a single step to the respective metal oxides. The results led to information about the composition, dehydration, ligand denticity and thermal decomposition of the isolated compounds.

1. Introduction

Tartaric acid (dihydroxybutanedioic acid) is an organic compound which has not an ample utilization as citric and malic acids, but it has a great importance in the provision industry. It is used as acidulant in some food [1].

Tartaric acid ($C_4H_6O_6$) is found in the grape in the form L(+) and among the organic acids of the grape, it is more strong [2].

A survey of the literature shows that the thermal studies involving compounds derivative of tartrate, reported the thermal decomposition and kinetics of dehydration of praseodymium (III), neodymium (III) and gadolinium (III) tartrates [3,4], TG and DSC studies on Sm(III) and Tb(III) tartrates [5], thermal decomposition behaviour of lanthanum (III), tris-tartrate lanthanide (III) decahydrate [6], studies on kinetics and mechanism of thermal decomposition of yttrium tartrate trihydrate crystals [7] and kinetics, mechanism of thermal decomposition of strontium tartrate crystals [8] and thermoanalytical study of some salts of 3d metals with tartaric acid [9–11].

In the present paper, solid-state compounds of bivalent manganese, iron, cobalt, nickel, copper and zinc with tartrate ($C_4H_4O_6{}^{2-}$) were prepared. The compounds were investigated by complexometry, elemental analysis, X-ray powder diffractometry, infrared spectroscopy, simultaneous thermogravimetry and differential thermal analysis (TG–DTA) and differential scanning calorimetry. The results allowed us to acquire information concerning these compounds in the solid-state including their thermal stability, ligand's denticity and crystallinity.

2. Experimental

The sodium tartrate dibasic dihydrate ($C_4H_4O_6Na_2{\cdot}2H_2O$) 99% purity was obtained from Sigma and aqueous solution 0.20 mol L^{-1} was prepared by direct weighing of the solid salt. Aqueous solutions of bivalent metal ions 0.20 mol L^{-1} were prepared by dissolving the corresponding chlorides.

The solid-state compounds were obtained by adding equivalent quantities of sodium tartrate to the respective metal chloride and the resulting solutions were heated and maintained in water bath until total precipitation of the metal tartrates. The precipitates were washed with hot distilled water until chloride ions were eliminated, filtered through and dried on Whatman no. 42 filtered papers, and kept in a desiccator over anhydrous calcium chloride. To avoid oxidation of Mn(II) and Fe(II), all their solutions as well as the water employed for washing their precipitates were purged with nitrogen gas, even in the solutions maintained in the water bath.

---

[*] Corresponding author.
E-mail address: emanuelbarretos@bol.com.br (E.C. Rodrigues).

0040-6031/$ – see front matter © 2009 Elsevier B.V. All rights reserved.
doi:10.1016/j.tca.2009.07.015

Table 1
Analytical data for the ML·nH$_2$O compounds.

Compound[a]	Metal oxide (%)			Ligand lost		Water (%)		Carbon (%)		Hydrogen (%)		Final
	Calcd.	TG	EDTA	Calcd.	TG	Calcd.	TG	Calcd.	E.A	Calcd.	E.A	Residue[b]
MnL·0.5H$_2$O	37.23	36.91	36.46	58.33	58.88	4.44	4.21	22.66	22.90	2.38	2.01	Mn$_2$O$_3$
FeL	39.16	38.8	38.77	60.84	61.20	–	–	23.56	23.70	1.98	1.61	Fe$_2$O$_3$
CoL·0.5H$_2$O	37.15	36.85	36.95	58.68	58.64	4.17	4.51	22.24	21.90	2.34	2.49	Co$_3$O$_4$
NiL·2.5H$_2$O	29.67	29.32	29.45	52.44	53.11	17.89	17.57	19.08	19.32	3.61	3.66	NiO
CuL	37.59	37.73	37.84	62.41	62.27	–	–	22.70	23.15	191	1.51	CuO
ZnL	38.12	38.03	37.82	61.88	61.97	–	–	22.51	22.40	1.89	2.11	ZnO

[a] L means tartrate.

[b] All the residues was confirmed by X-ray powder diffractometry.

In the solid-state compounds, metal ions, water and tartrate contents were determined from TG curves. The metal ions were also determined by complexometry with standard EDTA solutions [12,13] after igniting the compounds to the respective oxides and their dissolution in hydrochloric acid.

Simultaneous TG–DTA and DSC curves were obtained with two thermal analysis system, models SDT 2960 and Q 10, both from TA Instruments. The purge gas was an air flow of 150 mL min^{-1}. A heating rate of 20 °C min^{-1} was adopted, with samples weighing about 7–8 mg. Alumina and aluminum crucibles, the latter with perforated covers, were used for TG–DTA and DSC, respectively.

Carbon and hydrogen contents were determined by microanalytical procedures, with an EA 1110 CHNS-O Elemental Analyzer from CE Instruments.

X-ray powder patterns were obtained with a Siemens D-5000 X-ray diffractometer using Cu Kα radiation (λ = 1.544 Å) and settings of 40 kV and 20 mA.

Infrared spectra for tartrate (sodium salt) as well as for its metal ion compounds were run on a Nicolet model Impact 400 FTIR instrument, within the 4000–400 cm^{-1} range. The solid samples were pressed into KBr pellets.

3. Results and discussion

The analytical and thermoanalytical (TG) data are shown in Table 1. These results establish the stoichiometry of these compounds, which are in agreement with the general formula: ML·nH$_2$O, where M represents Mn(II), Fe(II), Co(II), Ni(II), Cu(II) or Zn(II), L is tartrate and n = 0 (Fe, Cu, Zn), 0.5 (Mn, Co) and 2.5 (Ni).

The X-ray diffraction powder patterns (Fig. 1) show that all the compounds have a crystalline structure, without evidence of the formation of isomorphous compounds.

Infrared spectroscopic data on tartrate and its compounds with the metal ions considered in this work are shown in Table 2. The investigation was focused mainly within the 1750–1000 cm^{-1} range because this region is potentially the most informative in attempting to assign coordination sites. The IR spectrum of acid shows a peak at 1743 cm^{-1} which is indicative of free carboxyl groups. The spectrum of the compounds show peaks at lower wavenumbers which is indicative of coordination carboxylate groups. The spectrum of tartaric acid also shows a peak at 1088 cm^{-1} indicative of a C–O stretching (alcohol group). The spectrum of the compounds also show a split or doublet bands, both shifted to lower frequencies in the complexes, namely 1092–1041 cm^{-1}, suggesting metals coordination by carboxylate with participation of the alcoholic hydroxyl groups of the ligand.

Simultaneous TG–DTA and DSC curves of the compounds are shown in Figs. 2–7. The TG–DTA curves show mass losses in a single or two steps, corresponding to endothermic peaks due to dehydration and exothermic ones attributed to the oxidation of organic matter. The thermoanalytical data of TG–DTA curves are shown in Table 3. The DSC curves also show endothermic and exothermic peaks, corresponding to the mass losses displayed by the TG curves. The differences observed concerning the peak temperature or the profiles of these curves are undoubtedly due to the perforated cover used to obtain the DSC curves, while the TG–DTA ones are obtained without cover.

The thermal stability of the anhydrous compounds (I) as well as the final temperature of thermal decomposition (II) as shown by the TG–DTA curves depend on the nature of the metal ion, and they

Table 2
Spectroscopic data.

	ν_{as} (COO$^-$)	ν_{sym} (COO$^-$)	ν_{ax} (C–O) alcohol
Acid	1743[*]		1088
Sodium salt	1619[s]	1410[m]	1113/1066
MnL·0.5H$_2$O	1608[s]	1412[m]	1084/1045
FeL	1587[s]	1404[m]	1086/1041
CoL·0.5H$_2$O	1616[s]	1415[m]	1086/1043
NiL·2.5H$_2$O	1608[s]	1398[m]	1086/1047
CuL	1623[s]	1365[m]	1074/1059
ZnL	1606[s]	1419[m]	1092/1049

ν_{sym} (COO−): symmetrical vibrations of the COO$^-$ group.
ν_{as} (COO−): anti-symmetrical vibrations of the COO$^-$ group.
ν_{ax} (C–O): axial stretching of C–O of the alcohol group.

[*] Free carboxyl groups.

[s] Strong.

[m] Medium.

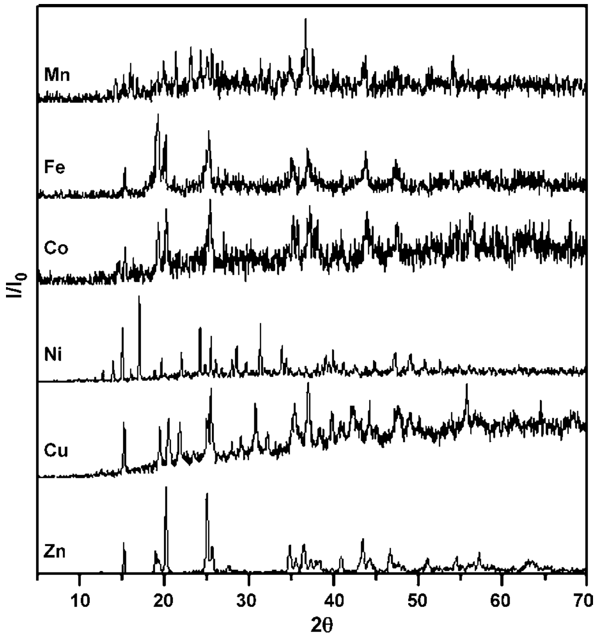

Fig. 1. X-ray powder diffraction patterns of the compounds: MnL·0.5H$_2$O; FeL; CoL·0.5H$_2$O; NiL·2.5H$_2$O; CuL and ZnL.

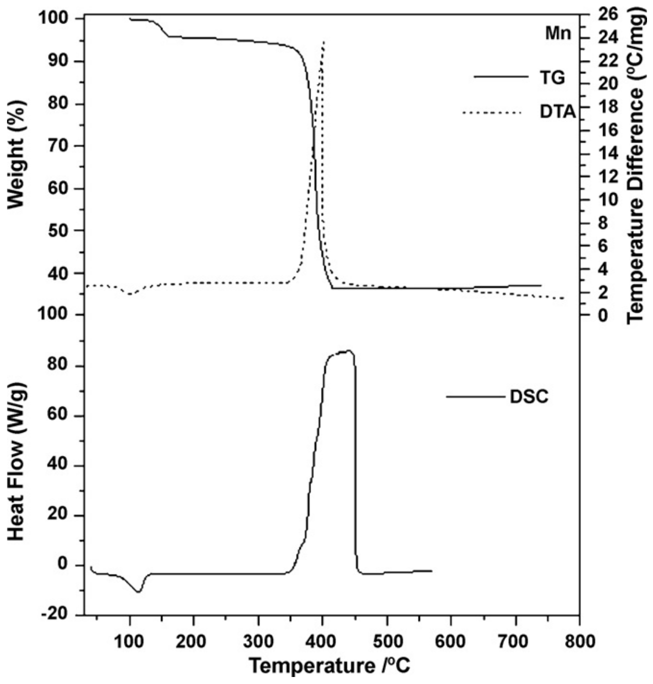

Fig. 2. TG–DTA and DSC curves of MnL·0.5H_2O (L = tartrate).

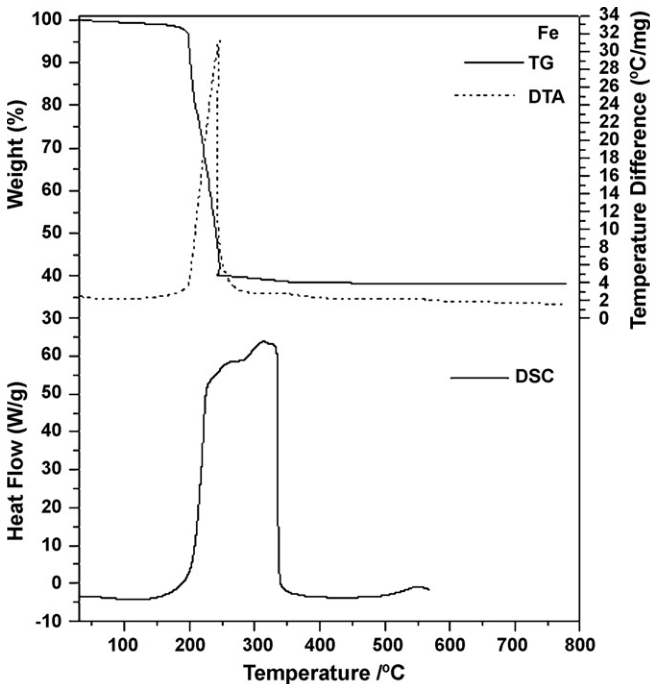

Fig. 3. TG–DTA and DSC curves of FeL (L = tartrate).

follow the order:

$$(\mathrm{I})\,\mathrm{and}\,(\mathrm{II}): \mathrm{Zn} > \mathrm{Mn}:\mathrm{Co} > \mathrm{Ni} > \mathrm{Fe} > \mathrm{Cu}.$$

The thermal behaviour of the compounds is heavily dependent on the nature of the metal ion and so the features of each of these compounds are discussed individually.

Manganese compound: The simultaneous TG–DTA and DSC curves are shown in Fig. 2. The first mass loss observed between 65 and 110 °C, corresponding to the endothermic peak at 100 °C (DTA) or 115 °C (DSC) is due to dehydration, with loss of 0.5H_2O (Calcd. = 4.44%; TG = 4.21%). The anhydrous compound is stable up to 315 °C and the thermal decomposition occurs in a single step between 350 and 460 °C (DSC) attributed to the oxidation of the organic matter. The total mass loss up to 405 °C is in agreement with the formation of Mn_2O_3, as final residue (Calcd. = 62.77%; TG = 63.09%) and confirmed by X-ray powder diffractometry. The residue at 420 °C is in agreement with Ref. [9]. However the decomposition to Mn_3O_4 was not observed.

Iron compound: The simultaneous TG–DTA and DSC curves are shown in Fig. 3. These curves show that the compound is anhydrous and stable up to 175 °C. Above this temperature the thermal decomposition occurs in two steps between 175–245 °C and 245–360 °C, with loss of 60.31% and 0.9% respectively corresponding to the large and sharp exothermic peak at 245 °C and small exothermic event at 340 °C (DTA) or the broad exotherm between 185 and 350 °C (DSC) attributed to the oxidation of Fe(II) to Fe(III) and organic matter.

Table 3
Temperature ranges (θ), mass losses or gain (%) and peak temperatures observed for each step of TG–DTA curves of the compounds.

Compound		TG–DTA steps			DSC peaks	
		First	Second	Third	First	Second
MnL·0.5H_2O[a]	θ/°C	65–110	315–405			
	Loss/%	4.21	58.88			
	Peak/°C	100 (endo)	400 (exo)		115 (endo)	350–460 (exo; broad)
FeL	θ/°C	175–245	245–360			
	Loss/%	60.31	0.9			
	Peak/°C	245 (exo)	340 (exo)		–	185–350 (exo; broad)
CoL·0.5H_2O	θ/°C	65–145	315–405			
	Loss/%	4.51	58.64			
	Peak/°C	100 (endo)	405 (exo)		107; 141 (endo)	350 – 475 (exo; broad)
NiL·2.5H_2O	θ/°C	75–140	310–370	370–650		
	Loss/%	17.57	70.33	0.35[b]		
	Peak/°C	130 (endo)	365 (exo)		144 (endo)	335–450 (exo; broad)
CuL	θ/°C	205–280	280–500			
	Loss/%	65.84	3.57[b]			
	Peak/°C	270 (exo)	–		–	220–390 (exo; broad)
ZnL	θ/°C	325–435	–			
	Loss/%	61.77	–			
	Peak/°C	415 (exo)	–		–	380–475 (exo; broad)

[a] L means tartrate.

[b] Mass gain.

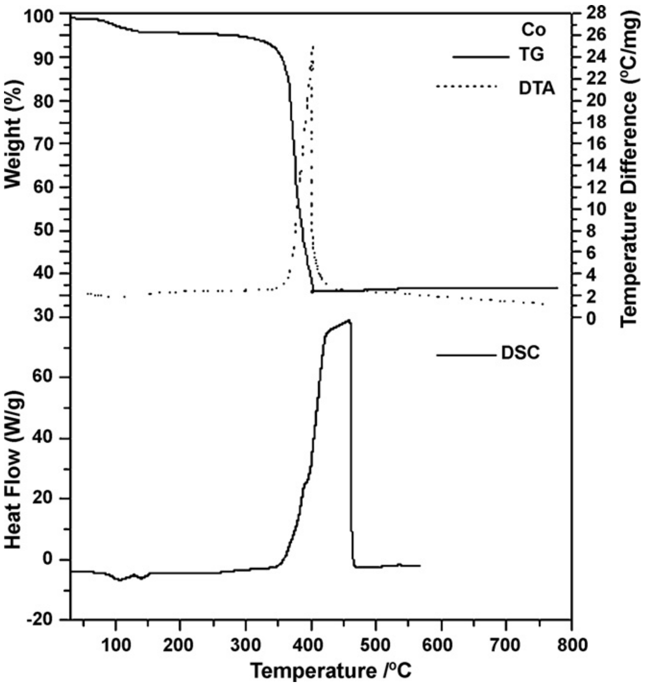

Fig. 4. TG–DTA and DSC curves of CoL·0.5H_2O (L = tartrate).

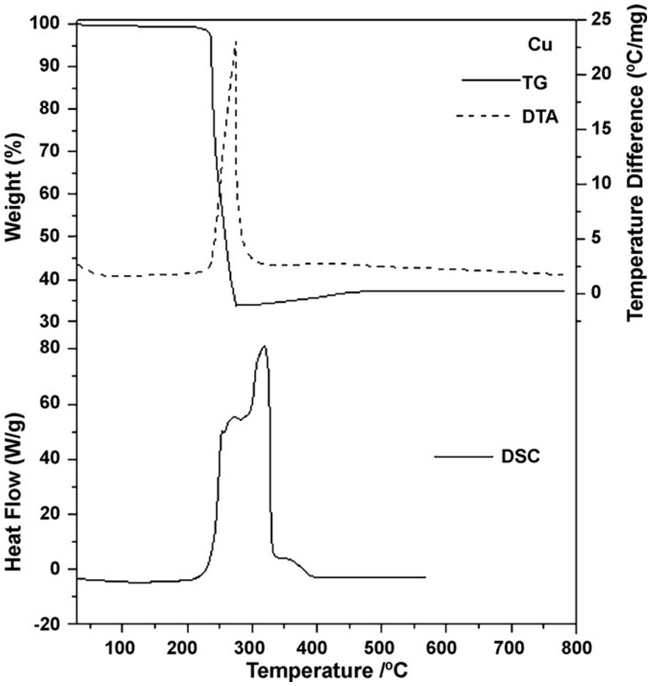

Fig. 6. TG–DTA and DSC curves of CuL (L = tartrate).

The profiles of the TG–DTA curves corresponding to the first mass loss show that the oxidation of the organic matter occurs with combustion. The total mass loss up to 360 °C is in agreement with the formation of Fe_2O_3, as final residue (Calcd. = 60.84%; TG = 61.20%) and confirmed by X-ray powder diffractometry. These results are in agreement with the thermal decomposition of the iron compound as described by Dranca [9] and Venkataraman [10].

Cobalt compound: The simultaneous TG–DTA and DSC curves are shown in Fig. 4. The mass loss that occurs between 65 and 145 °C, corresponding to small endothermic event at 100 and 130 °C (DTA) or 107 °C or 141 °C (DSC) is due to dehydration that occurs in two steps, with loss of 0.5H_2O (Calcd. = 4.17%; TG = 4.51%). The anhydrous compound is stable up to 315 °C and above this temperature the thermal decomposition occurs in a single step up to 405 °C with loss of 58.64%, corresponding to exothermic peak at 405 °C (DTA) or the broad exotherm between 350 and 475 °C (DSC), attributed to the oxidation of organic matter. The profiles of the TG–DTA curves also show that the oxidation of the organic matter occurs with combustion. The total mass loss up to 405 °C is in agreement with the formation of Co_3O_4, as final residue (Calcd. = 62.85%; TG = 63.15%) and confirmed by X-ray powder diffractometry. The results are in agreement with the literature [9]. However the formation of

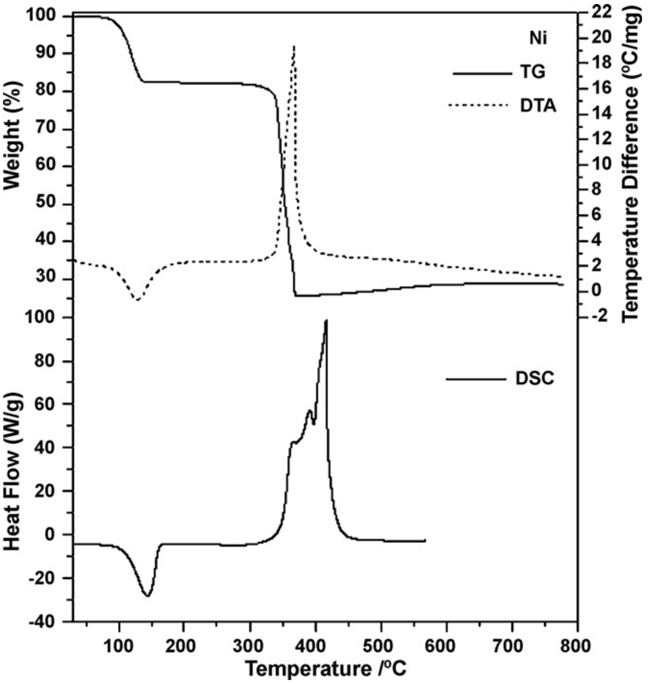

Fig. 5. TG–DTA and DSC curves of NiL·2.5H_2O (L = tartrate).

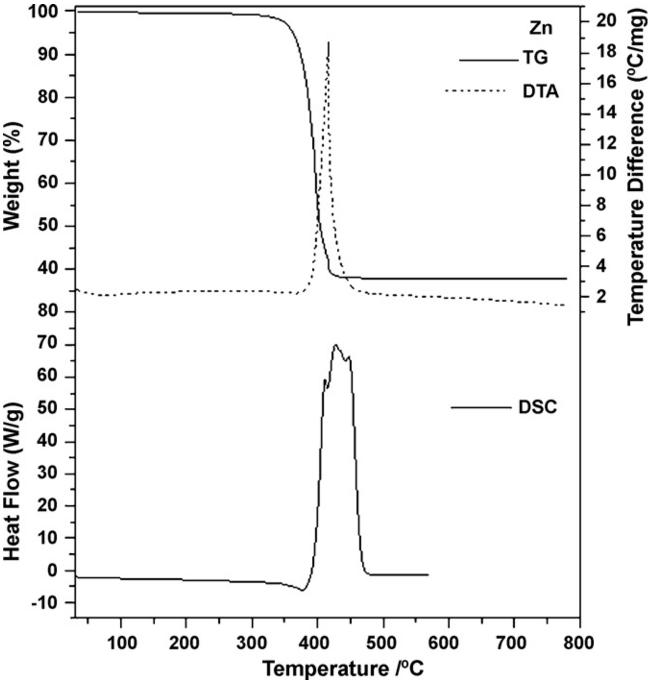

Fig. 7. TG–DTA and DSC curves of ZnL (L = tartrate).

stable anhydrous compound and the thermal decomposition of the anhydrous compound, without formation of intermediate are in disagreement with the results described in Ref. [11]. The disagreement undoubtedly is due to the different condition used for obtaining these curves, even for preparation the compound.

Nickel compound: The simultaneous TG–DTA and DSC curves are shown in Fig. 5. The first mass loss between 75 and 140 °C corresponding to the endothermic peak at 130 °C (DTA) or 144 °C (DSC) is due to dehydration, which occurs in a single step with loss of 2.5 H_2O (Calcd. = 17.89%; TG = 17.57%). The anhydrous compound is stable up to 310 °C and above this temperature the thermal decomposition occurs in a single step up to 370 °C with loss of 74.49% corresponding to the exothermic peak at 365 °C (DTA) or the broad exotherm between 335 and 450 °C (DSC) attributed to the oxidation of the organic matter. The total mass loss up to this step suggests the formation of a mixture of Ni and NiO, as residue. The mass gain observed between 370 and 650 °C, is attributed to oxidation of Ni to NiO, although no exothermic event due to this oxidation is observed in DTA curve, probably because the oxidation occurs through a slow process and the heat evolved is not enough to procedure the thermal event. The total mass loss up to 650 °C is in agreement with the formation of NiO, as final residue (Calcd. = 70.33%; TG = 70.68%) and confirmed by X-ray powder diffractometry.

Copper compound: The simultaneous TG–DTA and DSC curves are shown in Fig. 6. These curves show that the compound is anhydrous and stable up to 205 °C. Above this temperature the thermal decomposition occurs in a single step up to 280 °C with loss of 65.84%, corresponding to the exothermic peak at 270 °C (DTA) or the broad exotherm between 220 and 390 °C (DSC) attributed to oxidation of the organic matter. The mass loss up to this step is in agreement with the formation of Cu_2O as residue (Calcd. = 66.19%; TG = 65.84%).

The mass gain observed between 280 and 500 °C is attributed to the oxidation of Cu_2O to CuO, and as already observed in the nickel compound, no exothermic event due to this oxidation is also observed in the DTA curve. The total mass loss up to 500 °C is in agreement with the formation of CuO as final residue (Calcd. = 62.41%; TG = 62.27%) and confirmed by X-ray powder diffractometry.

Zinc compound: The simultaneous TG–DTA and DSC curves are shown in Fig. 7. These curves also show that the compound is anhydrous and stable up to 325 °C. Above this temperature the thermal decomposition occurs in a single step up to 435 °C, with loss of 61.77% corresponding to the exothermic peak at 415 °C (DTA) or the broad exotherm between 380 and 475 °C (DSC) attributed to oxidation of the organic matter. The total mass loss up to 435 °C is in agreement with the formation of ZnO, as final residue (Calcd. = 61.88%; TG = 61.77%) and confirmed by X-ray powder diffractometry.

Although the copper and zinc compound were obtained in anhydrous state the thermal decomposition of nickel, copper and zinc compound are in agreement with the literature [9]. Small difference in the TG–DTA profiles and the temperatures of thermal decomposition undoubtedly were due to different condition used for obtaining these curves.

4. Conclusion

From TG–DTA, complexometry and elemental analysis data, a general formula could be established for the compounds involving some bivalent metal ions and tartrate. The X-ray powder patterns pointed out that the synthesized compounds have a crystalline structure, without evidence concerning the formation of isomorphous series. The infrared spectroscopic data suggest that both carboxylic and alcoholic group act as coordination sites.

The TG–DTA and DSC curves provided previously unreported information about the thermal stability and thermal decomposition of these compounds.

Acknowledgements

The authors thank UNESP Postdoctoral Program and FAPESP, CNPQ, CAPES Foundations (Brazil) for financial support.

References

[1] T.W.G. Solomons, C. Fryhle, Organic Chemistry, eighth ed., LTC, São Paulo, 2005.
[2] L.A. Rizzon, A. Miele, Cienc. Rural 31 (2001) 893.
[3] R.M. Sharma, M.L. Kaul, J. Indian Chem. Soc. LXIV (1987) 459.
[4] R.M. Sharma, M.L. Kaul, J. Indian Chem. Soc. 67 (1990) 706.
[5] R.M. Sharma, M.L. Kaul, J. Thermal Anal. 35 (1989) 2143.
[6] N. Deb, J. Therm. Anal. Cal. 78 (2004) 227.
[7] K.K. Bamzai, S. Kuwar, Mater. Chem. Phys. 107 (2008) 200.
[8] S.K. Arora, V. Patel, A. Kothari, Mater. Chem. Phys. 84 (2004) 323.
[9] I. Dranca, T. Lupascu, V. Sofransky, V. Popa, M. Vass, J. Thermal Anal. 46 (1996) 1403.
[10] A. Venkataraman, V.A. Mukhedkar, A.J. Mukhedkar, J. Thermal Anal. 35 (1989) 2115.
[11] N.N. Dass, S. Sarmah, J. Therm. Anal. Cal. 58 (1999) 137.
[12] H.A. Flaschka, EDTA Titrations, Pergamon Press, Oxford, 1964.
[13] C.N. de Oliveira, M. Ionashiro, C.A.F. Graner, Ecl. Quim. 10 (1985) 7.